RSC Advances

PAPER

View Article Online
View Journal | View Issue

Cite this: *RSC Adv.*, 2024, **14**, 14640

Influence of alkali metal ions (K^+ and Na^+) on the preparation of magnesium hydroxide hexagonal flakes

Cunjian Weng,[a] Xuewen Song, *[b] Haibin Zhu[b] and Xianping Luo *[abc]

Magnesium hydroxide ($Mg(OH)_2$), as a green halogen-free flame retardant, has attracted significant attention in the field of flame retardant composite materials. In addition to conventional indicators such as purity and whiteness, $Mg(OH)_2$ is required to take the form of regular hexagonal sheets to ensure the dispersion of composite materials. We use irregular large particles of $Mg(OH)_2$ prepared by the magnesium factory in western Qinghai as raw materials to study the influence of alkali metal ions K^+ and Na^+ mainly present in salt lakes on the physicochemical properties of $Mg(OH)_2$. The products were characterized *via* X-ray diffraction, scanning electron microscopy, automatic nitrogen physical adsorption apparatus, and other modern characterization techniques. Results show that alkali metal ions K^+ and Na^+ considerably influence the crystal surface polarity, particle size, and morphology of the prepared $Mg(OH)_2$. The mechanism analysis shows that the presence of K^+ and Na^+ alters the dissolution, recrystallization, and growth characteristics of $Mg(OH)_2$. This study provides theoretical support for the realization of high-performance $Mg(OH)_2$ using salt lake resources and demonstrates the value for promoting the large-scale industrial application of the salt lake industry.

Received 12th January 2024
Accepted 22nd April 2024

DOI: 10.1039/d4ra00305e

rsc.li/rsc-advances

1. Introduction

$Mg(OH)_2$ is nontoxic and nonpolluting and exhibits high-temperature resistance, corrosion resistance, and other excellent physical and chemical properties.[1,2] Therefore, it is widely used as an antibacterial agent in wastewater[3–5] and waste gas, for the treatment of acidic water contaminants, for fillers in the paper industry,[6] in electronic and optical devices,[7,8] and as a precursor for producing magnesium oxide[9] and new generation flame retardants.[10–15] The physical and chemical properties of $Mg(OH)_2$ products, such as the morphology, particle size, particle size distribution, dispersion, specific surface area, whiteness, and purity, play a key role in their applications. The preparation of $Mg(OH)_2$ products not only requires their high purity but also necessitates the regulation of their physical and chemical properties, such as the particle size and morphology.[16,17] Despite significant research in this area, numerous challenges remain in the actual production and preparing high-performance $Mg(OH)_2$ is still a topic of interest at present.

The hydrothermal method is commonly employed to control nucleation growth of the $Mg(OH)_2$ crystal surface by regulating its dissolution and recrystallization.[18] Currently, the use of ultrasound, microwave-assisted technology,[19] and additives,[20] among other, to regulate $Mg(OH)_2$ formation during hydrothermal reactions is a hot topic. Further, the most commonly employed method involves regulating the nucleation, crystallization, and other growth processes of $Mg(OH)_2$ using various additives.[21] Gong *et al.*[22] showed that the presence of magnesium lactate can transfer hydroxyl groups from brucite to $Mg(OH)_2$ nanoplates, thereby acting as a conveyor belt. Gómez-Villalba[23] *et al.* showed that using hydrazine hydrate as a surfactant significantly affects the physical and chemical properties, especially the morphology, of the obtained $Mg(OH)_2$ products. According to literature, inorganic alkaline crystal surface regulators, such as NaOH, can provide sufficient OH^-[24] for $Mg(OH)_2$ recrystallization and thus rearrange its structure by taking advantage of the differences in the action of different polar crystal faces and OH^-[25] to control the crystal face orientation and particle size.[26] Although there have been some studies on the use of sodium hydroxide and potassium hydroxide as crystal regulators to regulate $Mg(OH)_2$ growth, no studies exist on alkali metal ions K^+ and Na^+ as additives. Hence, herein, we conducted a study on the effects of K^+ and Na^+ on the hydrothermal synthesis of $Mg(OH)_2$ with large and irregular particles. The study provides a great reference value for the preparation of high-performance $Mg(OH)_2$.

[a]*School of Materials Science and Engineering, Xi'an University of Architecture and Technology, Xi'an 710055, China*
[b]*School of Resource Engineering, Xi'an University of Architecture and Technology, Xi'an 710055, China. E-mail: Songxwhl@163.com*
[c]*School of Resources and Environmental Engineering, Jiangxi University of Science and Technology, Ganzhou 341000, China*

The influence of K^+ and Na^+ on the physical and chemical properties of prepared $Mg(OH)_2$ was studied using NaCl and KCl as crystal surface regulators and $Mg(OH)_2$ with large particles produced by the magnesium industry in western Qinghai as the raw material. Alkali metal ions K^+ and Na^+ were used to regulate the dissolution and recrystallization of $Mg(OH)_2$, related crystal growth mechanism was discussed, and low-polarity $Mg(OH)_2$ hexagonal flakes were prepared. This study has important theoretical and practical significance for the preparation of flame retardants using high-performance $Mg(OH)_2$ hexagonal flakes.

2. Material and methods

2.1. Materials

KCl and NaCl were procured from Xilong Science Co, LTD. Purified water was prepared in the laboratory. $Mg(OH)_2$ with large particles was produced by the magnesium industry in western Qinghai was used as the raw material; its morphology, particle size distribution, and crystal phase composition are shown in Fig. 1.

2.2. Experimental methods

A total of 40 g of $Mg(OH)_2$ (0.69 mol) and a certain amount of NaCl and KCl were weighed and added into a high-temperature, high-pressure reactor along with 160 mL purified water. Hydrothermal heat treatment was then performed at 500 r min^{-1} with varying additive concentration (namely KCl and NaCl concentration), reaction temperature, and reaction time. After the reaction was completed, the $Mg(OH)_2$ cake was washed using an ethanol solution to neutralize it, dried at 105 °C for 6 h, and the obtained $Mg(OH)_2$ product was sealed for subsequent characterization and analysis.

2.3. Characterization analysis test

Several analytical techniques were used to characterize the obtaine powders.

X-ray powder Diffraction. The resulting powder crystalline phases were carried out using X-ray diffraction (XRD, DX-2700BH). A Cu Kα source was used over a 2θ range of 20° to 60° and a step size of 0.02° with a dwell time of 0.05 s was applied during the analyses.

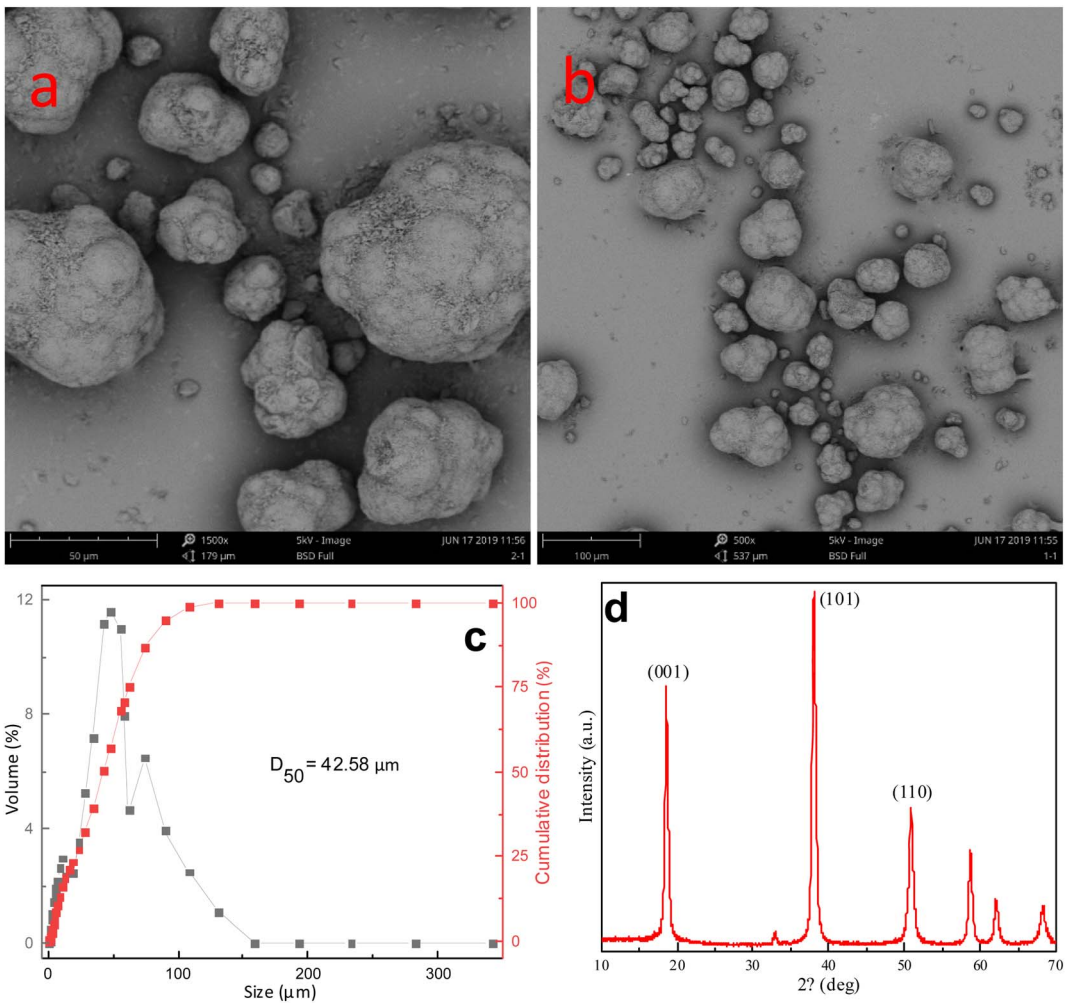

Fig. 1 Morphology, particle size distribution, and crystal phase composition of $Mg(OH)_2$ products produced by the magnesium industry in western Qinghai. ((a and b): SEM images; (c): particle size distribution and cumulative distribution; and (d): XRD pattern).

Scanning Electron Spectroscopy (SEM). The particle shape and size were analyzed by scanning electron microscopy (SEM, SU8010). The powder samples for SEM were shown and observed at a working distance of 3.5 mm and a stimulation voltage of 0.7 kV.

Dynamic light scattering (DLS). Using the dynamic light scattering method, the obtained $Mg(OH)_2$ particle, D50 size, and particle size distribution were researched by laser particle size analysis (OMCC, SCF-106A).

Brunauer–Emmett–Teller (BET). N_2 adsorption–desorption isotherms are recorded on a Micro Active for ASAP 2460 Version 2.02 at 77.300 K. N_2 adsorption–desorption isotherm (ASAP2460) is employed to analyze pore structure and surface area of $Mg(OH)_2$. Before the test, the samples are degassed overnight at 180 °C.

3. Results and discussion

The crystal phases and crystallinity of $Mg(OH)_2$ were determined *via* X-ray diffraction. Fig. 2 shows the X-ray diffraction (XRD) pattern of $Mg(OH)_2$ samples prepared at 160 °C in 6 h using different Na^+ concentrations. These XRD patterns exhibit typical diffraction peaks, which were assigned to (001), (100), (101), (102), and (110) planes of the structure of $Mg(OH)_2$. No additional XRD peaks arising from impurities were detected. As shown in Fig. 2, the strongest (*hkl*) peaks are located at 2θ values of 18.60°, 38.02°, and 50.84°, and the corresponding (*hkl*) index is as follows: (001), (101), and (102) are the main peaks of (001), (101) and (102) of $Mg(OH)_2$, respectively. The diffraction peak appears at 2θ value 58.66, corresponding to the $Mg(OH)_2$ crystal phase plane (110). The presence of Na^+ has an impact on the strength of the obtained $Mg(OH)_2$ crystal face. With the increasing content of Na^+, the strength of the (001) crystal face of the obtained $Mg(OH)_2$ product first increases and then decreases.

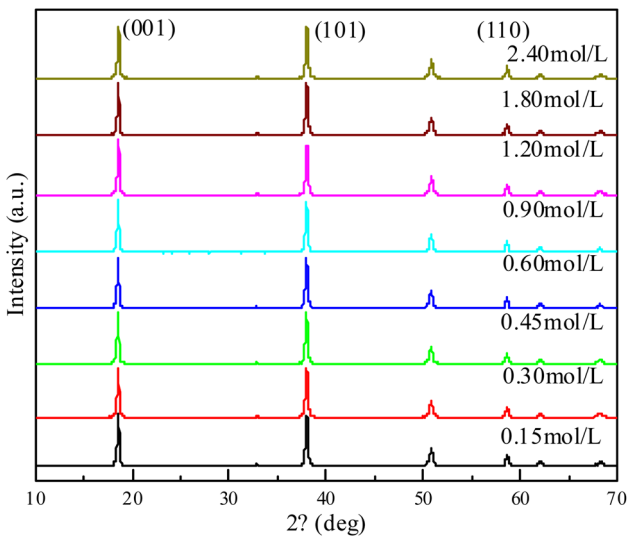

Fig. 2 $Mg(OH)_2$ products prepared using different Na^+ concentrations (reaction time: 6 h; reaction temperature: 160 °C).

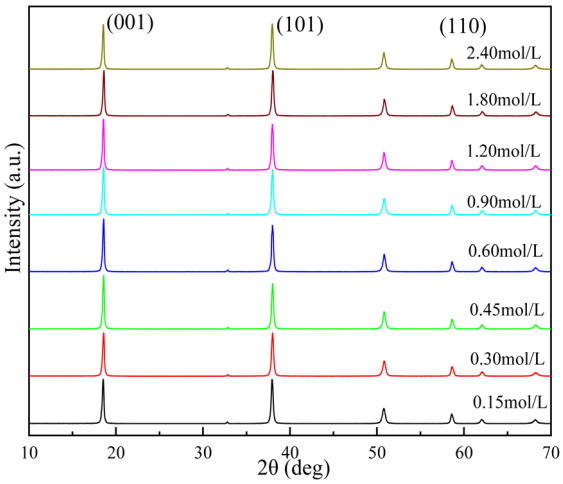

Fig. 3 $Mg(OH)_2$ products with different concentrations of K^+ (reaction time: 6 h; reaction temperature: 160 °C).

The $Mg(OH)_2$ crystal phases and crystallinity were determined by XRD. Fig. 3 shows the XRD pattern of $Mg(OH)_2$ samples prepared at a synthesis temperature of 160 °C and a synthesis time of 6 h in the presence of different concentrations of K^+. These XRD patterns exhibit typical diffraction peaks assigned to (001), (100), (101), (102), and (110) planes of the structure of $Mg(OH)_2$. No additional XRD peaks arising from impurities were detected. The strongest (*hkl*) peak detected is located at 2θ values of 18.60, 38.02, and 50.84, and the corresponding (*hkl*) index is as follows: (001), (101), and (102) are the main peaks of (001), (101) and (102) of $Mg(OH)_2$, respectively. The diffraction peak appears at 2θ value 58.66, corresponding to the $Mg(OH)_2$ crystal phase plane (110). The presence of K^+ has an impact on the strength of the obtained $Mg(OH)_2$ crystal face. With the increase in K^+ content, the crystal face of the obtained $Mg(OH)_2$ product first increases and then decreases.

Fig. 2 and 3 show that the increase in the concentration of K^+ and Na^+ leads to an increase and subsequent decrease of the intensity of (001), (101), and (110) diffraction peaks, with the intensity being the highest when the concentration of K^+ and Na^+ is 0.45 mol L^{-1}. This is attributed to less H^+ generated by hydrolysis when K^+ and Na^+ concentration is low, leading to a slower dissolution of $Mg(OH)_2$, which is not conducive to the dissolution-crystallization of Mg^{2+} on the surface of $Mg(OH)_2$, which hinders crystal growth. At high concentrations of K^+ and Na^+, hydrolysis releases more H^+ and the pH of the system is maintained at a low level, which is also not conducive to crystal growth.[27] Furthermore, due to the charge neutralization effect of anionic flocculants on $Mg(OH)_2$ and positive charge on the surface of $Mg(OH)_2$, Cl^- introduced by NaCl and KCl combines with $Mg(OH)_2$ more rapidly, further accelerating the dissolution of $Mg(OH)_2$.[28] Simultaneously, there is a higher number of impurity ions (Cl^-) in the solution, which affects the ordered crystallization of Mg^{2+} on the crystal surface of $Mg(OH)_2$ and reduces the integrity of crystal growth.

Fig. 4a shows that I_{001}/I_{101}, and I_{001}/I_{110} first increase and then decrease with increasing NaCl and KCl concentrations.

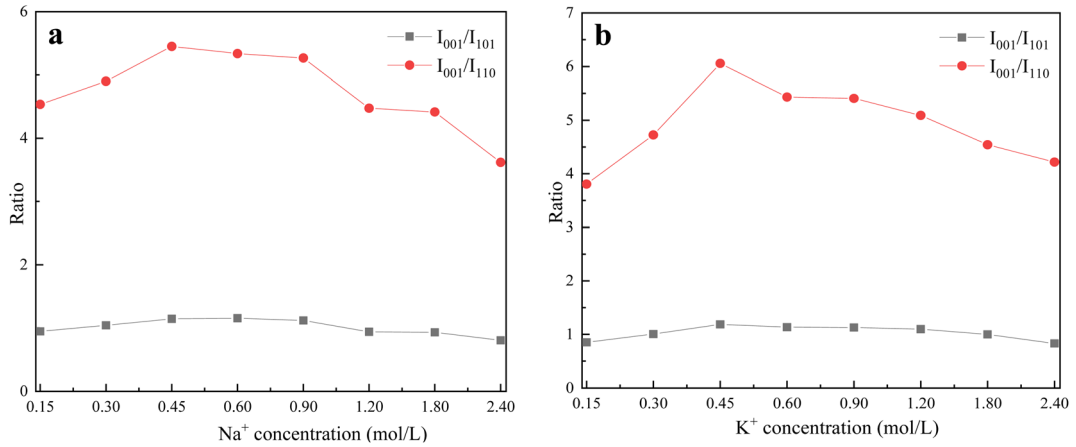

Fig. 4 XRD characteristic peak ratio of $Mg(OH)_2$ products at different Na^+ and K^+ concentrations ((a): Na^+; (b): K^+).

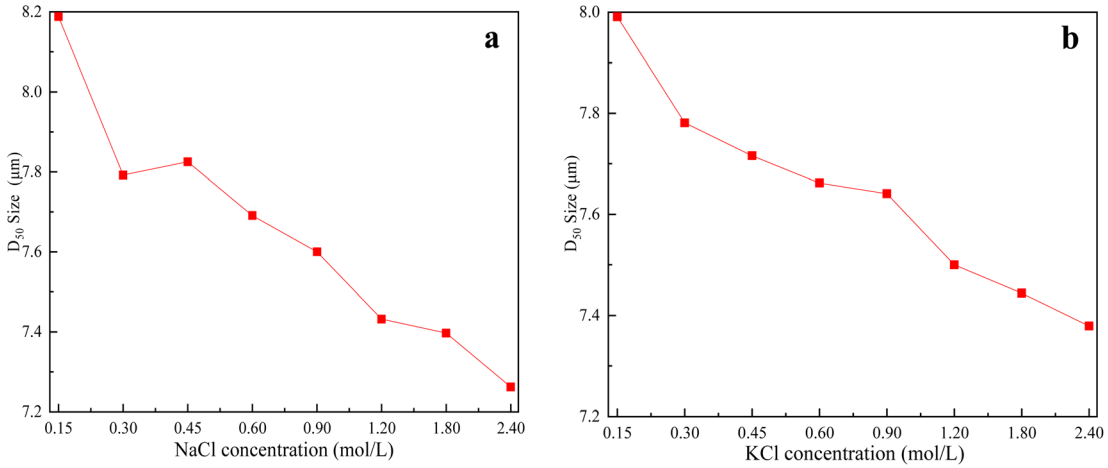

Fig. 5 D_{50} particle size variations of $Mg(OH)_2$ products at different Na^+ and K^+ concentrations ((a): Na^+; (b): K^+).

When K^+ and Na^+ concentration is 0.45 mol L^{-1}, I_{001}/I_{101} reaches its maximum. This shows that K^+ and Na^+, as crystal surface regulators, promote the selective growth of the (001) crystal surface. However, when K^+ and Na^+ concentration is low, the dissolution efficiency of $Mg(OH)_2$ decreases and the growth rate of the (001) crystal plane is lower than those of the (101) and

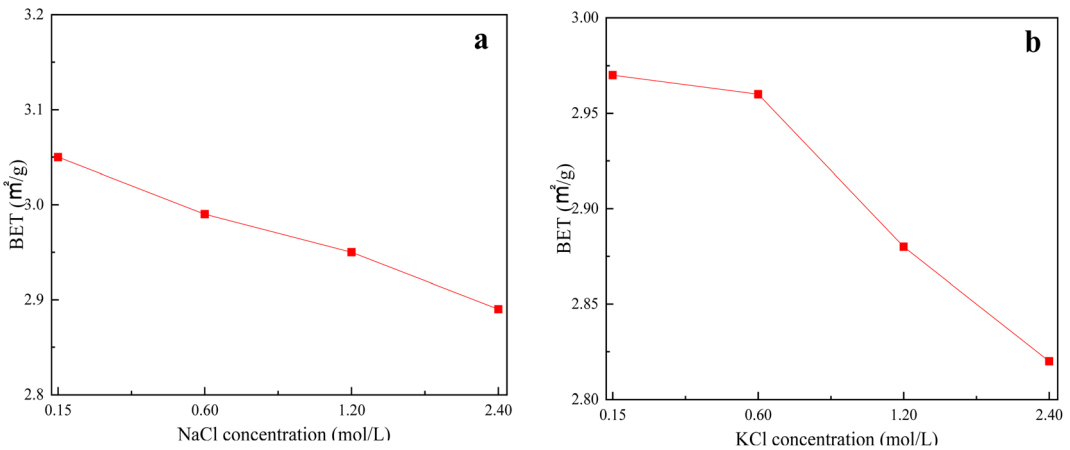

Fig. 6 BET changes of $Mg(OH)_2$ products at different Na^+ and K^+ concentrations ((a): Na^+; (b): K^+).

(110) crystal planes. When the crystal-surface-regulator concentration is high, excess Cl^- is introduced, which has a significant influence on the growth of the (001) crystal surface. We conclude that the concentrations of K^+ and Na^+, the crystal surface regulators, have a significant influence on the selective growth of the $Mg(OH)_2$ crystal surface. The increase in I_{001}/I_{101} and I_{001}/I_{110} may be attributed to the positive charge on the surface of the $Mg(OH)_2$ particles, which easily adsorb anions. As the radius of OH^- is smaller than that of the Cl^- in the precipitation system,[29] OH^- is more easily adsorbed onto the basic crystal plane of microcrystals and promotes the growth of particle edges. Thus, K^+ and Na^+ promote the growth of $Mg(OH)_2$ edges by providing Cl^- and improve the growth of the (001) crystal surface.[30]

Fig. 5 shows the variation in the particle size D_{50} of $Mg(OH)_2$ products prepared using different concentrations of NaCl and KCl. As shown in Fig. 5a, when the Na^+ concentration in the reaction system increases from 0.15 to 2.40 mol L^{-1}, the particle size of the obtained $Mg(OH)_2$ products increases from 8.18 μm dropped to 7.26 μm. Similarly, as shown in Fig. 5b, when the concentration of K^+ in the reaction system increases from 0.15 to 2.40 mol L^{-1}, the particle size of the obtained $Mg(OH)_2$ products increases from 7.99 μm dropped to 7.38 μm. We conclude that the increasing concentration of K^+ and Na^+ leads to a decrease in the particle size of the obtained $Mg(OH)_2$ products. Thus, the presence of K^+ and Na^+ has a significant effect on the dissolution and recrystallization of $Mg(OH)_2$, resulting in a continuous decrease in the particle size of the obtained products.

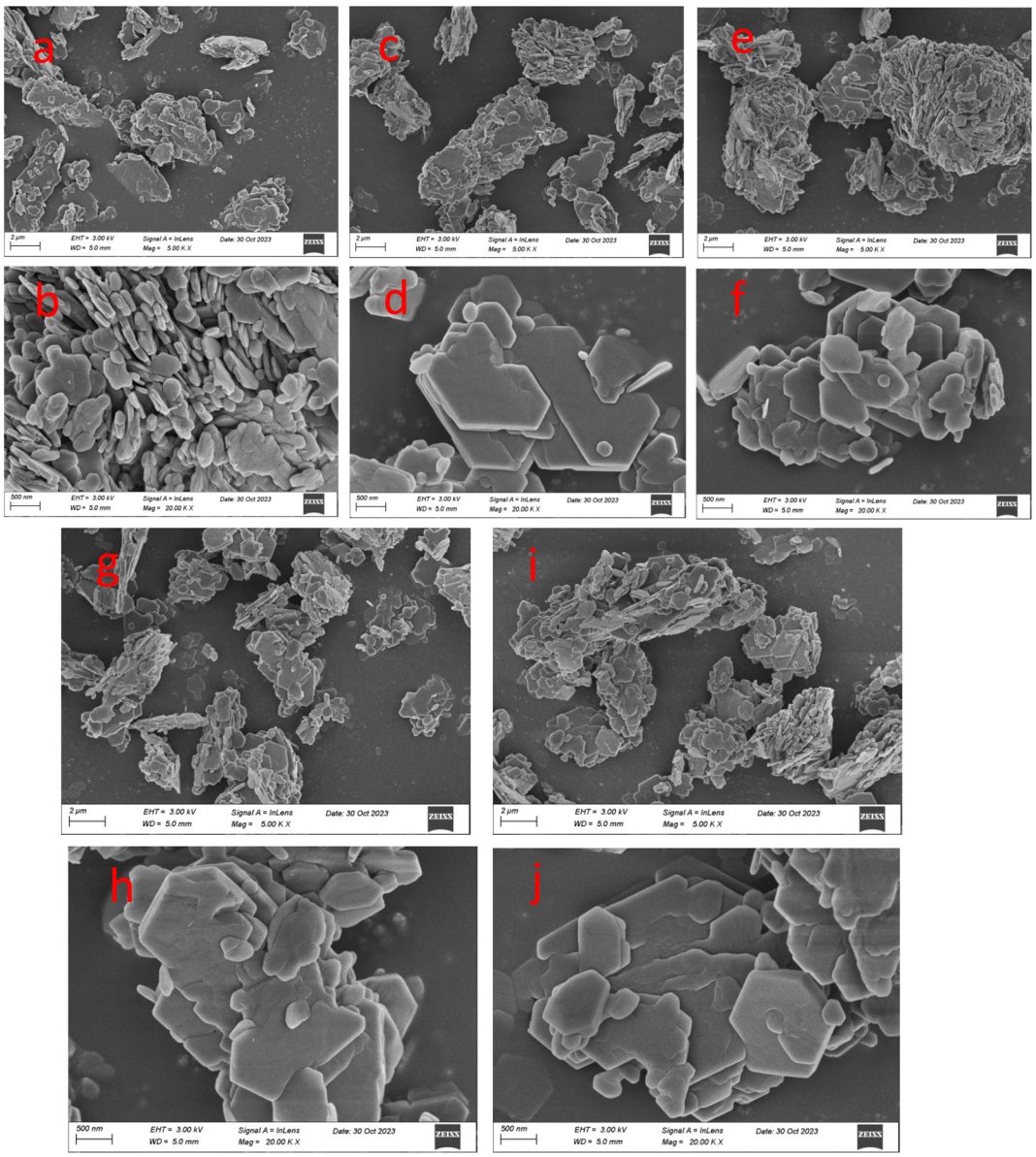

Fig. 7 Morphology of $Mg(OH)_2$ products prepared using different concentrations of Na^+ ((a and b): 0.15 mol L^{-1}; (c and d): 0.30 mol L^{-1}; (e and f): 0.60 mol L^{-1}; (g and h): 1.20 mol L^{-1}; (i, j and k): 2.40 mol L^{-1}).

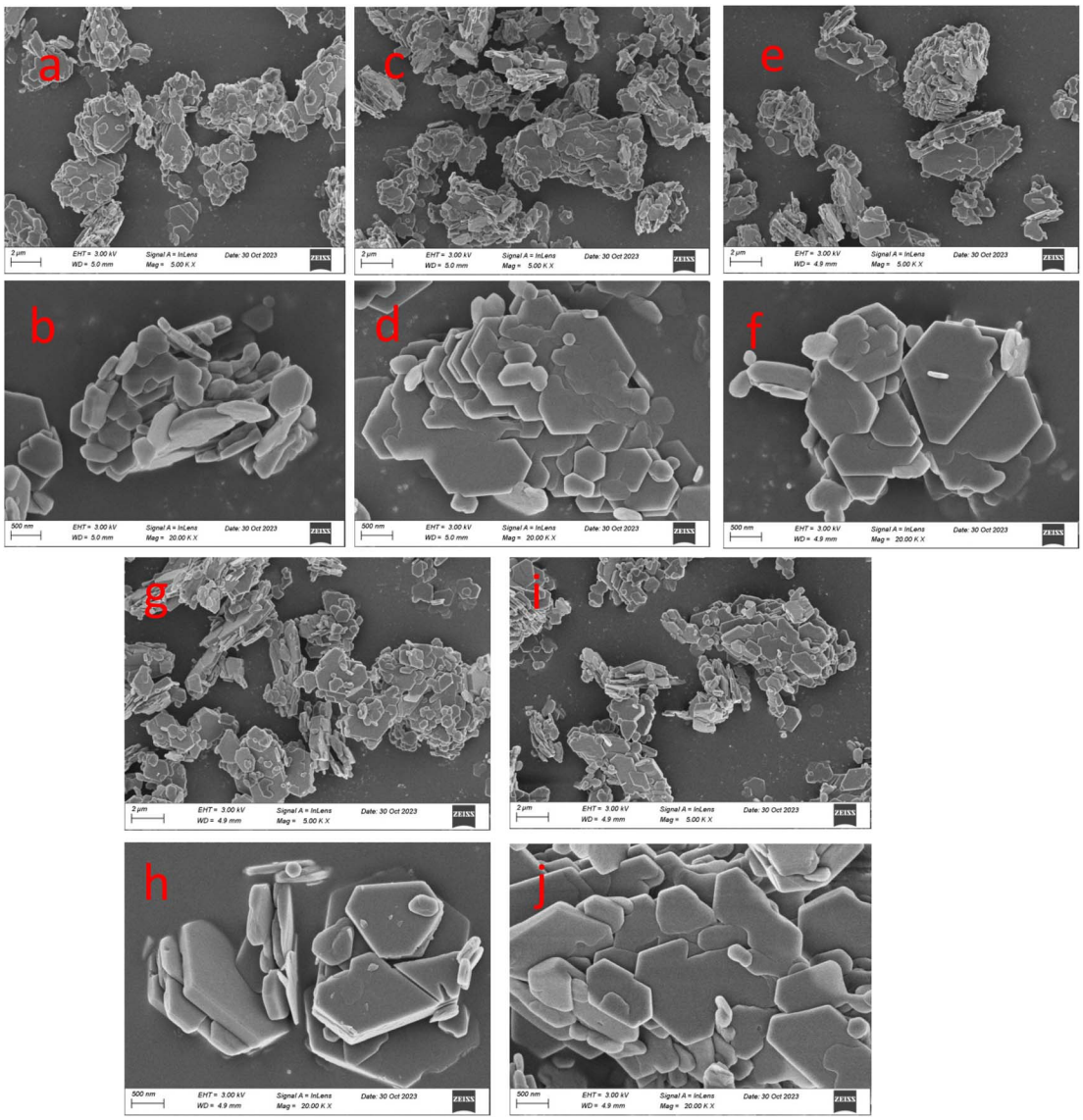

Fig. 8 Morphology of $Mg(OH)_2$ products prepared using different K^+ concentrations ((a and b): 0.15 mol L^{-1}; (c and d): 0.30 mol L^{-1}; (e and f): 0.60 mol L^{-1}; (g and h): 1.20 mol L^{-1}; (i, j and k): 2.40 mol L^{-1}).

Fig. 6 shows the BET changes of $Mg(OH)_2$ products obtained using different K^+ and Na^+ concentrations. With an increase in Na^+ concentration from 0.15 to 2.40 mol L^{-1}, the specific surface area of the obtained $Mg(OH)_2$ product decreases from 3.05 to 2.89 $m^2\ g^{-1}$ (Fig. 6a). With an increase in K^+ concentration from 0.15 to 2.40 mol L^{-1}, the specific surface area of the obtained $Mg(OH)_2$ product decreases from 2.97 to 2.82 $m^2\ g^{-1}$ (Fig. 6b). The continuous increase of alkali metal ions K^+ and Na^+ causes the specific surface area of the obtained $Mg(OH)_2$ product to decreases continuously, albeit the decrease is small. This may be attributed to the small polarity of the obtained $Mg(OH)_2$ product under these conditions, such that the presence of alkali metal ions K^+ and Na^+ has a relatively small impact on the specific surface area of $Mg(OH)_2$.

Fig. 7 and 8 show SEM images of $Mg(OH)_2$ products obtained in the presence of different concentrations of alkali metal ions K^+ and Na^+. The products obtained under these conditions are all hexagonal $Mg(OH)_2$ products. Compared with the morphology of the products obtained in Fig. 1, the morphology was subjected a significant change from irregular large particle $Mg(OH)_2$ to regular hexagonal flake $Mg(OH)_2$. This indicates that different concentrations of alkali metal ions K^+ and Na^+ play an important in the dissolution and recrystallization process of $Mg(OH)_2$, influencing the morphology of the obtained products.

4. Conclusions

Herein, we studied the influence of alkali metal ions K^+ and Na^+ as crystal surface regulators on the hydrothermal dissolution and recrystallization of $Mg(OH)_2$. The results show that the presence of K^+ and Na^+ has a significant effect on the crystal

structure, polarity, and particle size of the $Mg(OH)_2$ products. Under specific hydrothermal conditions, K^+ and Na^+ play a major role in controlling the selective growth of low-polarity crystal planes of $Mg(OH)_2$. The polarity ratio of the $Mg(OH)_2$ products prepared using Na^+ decreased from the highest value of 1.19 to 0.83. When the concentration of NaCl in the reaction system increases from 0.15 to 2.40 mol L^{-1}, the particle size of the obtained $Mg(OH)_2$ products increases from 8.18 μm dropped to 7.26 μm. Similarly, an increase in the concentration of K^+ in the reaction system from 0.15 to 2.40 mol L^{-1} leads to an increase in the particle size of the obtained $Mg(OH)_2$ products from 7.99 μm dropped to 7.38 μm. K^+ and Na^+ promote the transformation of irregular large particles of $Mg(OH)_2$ products into regular hexagonal flakes under hydrothermal conditions. This study provides theoretical support for the preparation of hexagonal flakes of high-performance $Mg(OH)_2$.

Conflicts of interest

There are no conflicts to declare.

Acknowledgements

This work was partially supported by the Open Project of Salt Lake Chemical Engineering Research Complex, Qinghai University (2023-DXSSKF-01), the National Key Research and Development Program of China (2022YFC2904305) and Major Science and Technology Projects of Qinghai Province (2020-GX-A1).

References

1 C. Dong, J. Cairney, Q. Sun, *et al.*, Investigation of Mg(OH)2 nanoparticles as an antibacterial agent, *J. Nanopart. Res.*, 2010, **12**, 2101–2109.
2 W. K. Jung, H. C. Koo, K. M. Kim, *et al.*, Antibacterial activity and mechanism of action of silver ion in Staphylococcus aureus and Escherichia coli, *Appl. Environ. Microbiol.*, 2008, **74**(7), 2171–2178.
3 H. Li, S. Liu, J. Zhao, *et al.*, Removal of reactive dyes from wastewater assisted with kaolin clay by magnesium hydroxide coagulation process, *Colloids Surf., A*, 2016, **494**, 222–227.
4 K. Wang, J. Zhao, H. Li, *et al.*, Removal of cadmium (II) from aqueous solution by granular activated carbon supported Mg(OH)2, *J. Taiwan Inst. Chem. Eng.*, 2016, **61**, 287–291.
5 M. El Bouraie and A. A. Masoud, Adsorption of phosphate ions from aqueous solution by modified bentonite with magnesium hydroxide Mg(OH)2, *Appl. Clay Sci.*, 2017, **140**, 157–164.
6 R. Giorgi, C. Bozzi, L. Dei, *et al.*, Nanoparticles of Mg(OH)2: synthesis and application to paper conservation, *Langmuir*, 2005, **21**(18), 8495–8501.
7 H. Y. Zahran, S. S. Shneouda, I. S. Yahia, *et al.*, Facile and rapid synthesis of nanoplates Mg(OH)2 and MgO via Microwave technique from metal source: structural, optical and dielectric properties, *J. Sol-Gel Sci. Technol.*, 2018, **86**, 104–111.
8 S. Yousefi, B. Ghasemi, B. Tajally, *et al.*, Optical properties of MgO and Mg(OH)2 nanostructures synthesized by a chemical precipitation method using impure brine, *J. Alloys Compd.*, 2017, **711**, 521–529.
9 L. Kumari, W. Z. Li, C. H. Vannoy, *et al.*, Synthesis, characterization and optical properties of Mg(OH)2 micro-/nanostructure and its conversion to MgO, *Ceram. Int.*, 2009, **35**(8), 3355–3364.
10 X. Kong, S. Liu and J. Zhao, Flame retardancy effect of surface-modified metal hydroxides on linear low density polyethylene, *J. Cent. South Univ. Technol.*, 2008, **15**(6), 779–785.
11 A. B. Morgan and C. A. Wilkie, *Flame Retardant Polymer Nanocomposites*, John Wiley &Sons, 2007.
12 X. Hui and X. Deng, Preparation and properties of superfine Mg(OH)2 flame retardant, *Trans. Nonferrous Met. Soc. China*, 2006, **16**(2), 488–492.
13 Y. Hu and S. Li, The effects of Mg(OH)2 on flash pyrolysis of polystyrene, *J. Anal. Appl. Pyrolysis*, 2007, **78**(1), 32–39.
14 H. Balakrishnan, A. Hassan, N. A. Isitman, *et al.*, On the use of magnesium hydroxide towards halogen-free flame-retarded polyamide-6/polypropylene blends, *Polym. Degrad. Stab.*, 2012, **97**(8), 1447–1457.
15 Y. Liany, A. Tabei, M. Farsi, *et al.*, Effect of nanoclay and magnesium hydroxide on some properties of HDPE/wheat straw composites, *Fibers Polym.*, 2013, **14**(2), 304–310.
16 P. Cheng, X. LI, B. Y. PEI, *et al.*, Influence mechanism of anions on growth and morphology of Mg(OH)2 crystal, *CIESC J.*, 2017, **68**(10), 3985–3992.
17 X. Hui and X. Deng, Preparation and properties of superfine Mg(OH)2 flame retardant, *Trans. Nonferrous Met. Soc. China*, 2006, **16**(2), 488–492.
18 L. S. Gómez-Villalba, A. Sierra-Fernández, O. Milosevic, *et al.*, Atomic scale study of the dehydration/structural transformation in micro and nanostructured brucite (Mg(OH)2) particles: Influence of the hydrothermal synthesis conditions, *Adv. Powder Technol.*, 2017, **28**(1), 61–72.
19 W. Shu-Yu, H. Wen-Zhi, L. Chang, *et al.*, Characterizations and preparation of Mg(OH)2 nanocrystals through ultrasonic–hydrothermal route, *Res. Chem. Intermed.*, 2016, **42**, 4135–4145.
20 J. Du, Z. Chen, Y. L. Wu, *et al.*, The effects of solvent and microwave on the preparation of Magnesium Oxide Precursor, *Cryst. Res. Technol.*, 2014, **49**(12), 959–964.
21 B. Jia and L. Gao, Morphology transformation of nanoscale magnesium hydroxide: from nanosheets to nanodisks, *J. Am. Ceram. Soc.*, 2006, **89**(12), 3881–3884.
22 W. Gong, D. Wu, Z. Cheng, *et al.*, Direct synthesis of porous Mg(OH)2 nanoplates from natural brucite, *Mater. Res. Bull.*, 2013, **48**(3), 1333–1337.
23 L. S. Gómez-Villalba, A. Sierra-Fernández, O. Milosevic, *et al.*, Atomic scale study of the dehydration/structural transformation in micro and nanostructured brucite (Mg(OH)2) particles: Influence of the hydrothermal

synthesis conditions, *Adv. Powder Technol.*, 2017, **28**(1), 61–72.

24 W. H. Lai, Y. X. Wang, Y. Wang, *et al.*, Morphology tuning of inorganic nanomaterials grown by precipitation through control of electrolytic dissociation and supersaturation, *Nat. Chem.*, 2019, **11**(8), 695–701.

25 P. Bhatt, S. Chattopadhyay, K. P. Misra, *et al.*, Effect of temporal pH variation of the reaction mixture on Mg(OH)2 morphology precipitated from an aqueous Mg(NO3)2-NaOH system, *Adv. Powder Technol.*, 2021, **32**(7), 2289–2299.

26 L. L. Jiao, P. C. Zhao, Z. Q. Liu, *et al.*, Preparation of magnesium hydroxide flame retardant from hydromagnesite and enhance the flame retardant performance of EVA, *Polymers*, 2022, **14**(8), 1567.

27 V. Berezovets, A. Kytsya, I. Zavaliy, *et al.*, Kinetics and mechanism of MgH2 hydrolysis in MgCl2 solutions, *Int. J. Hydrogen Energy*, 2021, **46**(80), 40278–40293.

28 S. L. Gou, X. Y. Nai, J. F. Xiao, *et al.*, Preparation and thermal decomposition of basic magnesium chloride whiskers, *J. Inorg. Mater.*, 2019, **34**(7), 781–785.

29 F. G. Yan, The Study on the Influence Factors of Hydration and Hydrothermal Processes to a Series of Magnesium Compound products, PhD thesis, East China Normal University, Shanghai, 2019.

30 Y. W. Cao, Y. Liu, H. M. Kong, *et al.*, Selective growth control and mechanism analysis of Mg(OH)2 low-polarity crystal surfaces, *Fine Chem.*, 2022, **39**(10), 2035–2043.